Study on dynamic behaviors of a breakwater triggered by earthquakes

Jie Lai[1], Yun Liu[1,2], Wei Wang[1], Chen-qiang Gao[1] , Zi-rong Niu[1], and Hai-bo Zhu[1]

1 Xi'an Research Institute of High-Tech, Xi'an 710025, China
2 Faculty of Architechtural and Enviromental Engineering, Chongqing industry polytechnic college, Chongqing 401120, China
E-mail: 513516059@qq.com

Abstract. To ensure the safety requirement of an artificial island in the construction period, the modified Hardin-Drnevich dynamic constitutive model and strength reduction method was used to analyze the dynamic response of a breakwater under the action of earthquakes. Research indicates the following: (1) the modified Hardin-Drnevich can effectively simulate the soil stress-strain relationship under dynamic action, and obtain strain hysteresis, and get permanent deformation of material; (2) the deeper the buried depth of breakwater, the greater soil pressure; (3) dynamic pressure response is more obvious on both sides of the breakwater at peak time in earthquakes.

1. Introduction

Artificial islands are located at sea, and as such represent complex environments, subject to the potentially adverse effects such as waves, ocean currents, wind, ice, and earthquakes. Breakwaters are important enclosure structures designed to protect artificial islands, and an instability of a breakwater will have catastrophic consequences for the artificial island it is built upon.

China's rapid economic development has brought strain upon land transportation networks. This, when coupled with its long coastline and numerous islands, means the development of coastal traffic has important political and economic significance. Coastal breakwaters in China are near the Circum–Pacific belt; hence, earthquakes happen frequently. These conditions can create numerous problems in engineering, so research in this area is of great significance for the construction of stable, effective breakwaters. As large-scale breakwater projects are in the initial development stages, the related research into breakwaters mainly focuses on construction technologies such as sandy soil liquefaction and static stability analysis [1-5]. WANG [6] applied the nonlinear constitutive model of a multiple shear mechanism type and calculated the effect of rotation of principal stress axis direction.

Matsuda, et al. [7] proposed the damage mechanism of breakwaters during earthquake–tsunami events, in which a simulated breakwater was destabilized by not only wave pressure, but also long-acting tsunami seepage flow and overflow.

However, the dynamic stability of breakwaters has not been fully investigated, which may mean the stability requirements are not being met in engineering practices. Based on this concern, a breakwater project in the East China Sea is analyzed in this paper by a strength reduction approach, taking into account the effects of seepage, earthquakes, pore water pressure, and other factors. These research results would provide an important reference for engineering construction.

Further, the dynamic characteristics and stability of this breakwater are studied by considering the coupled actions of seepage, earthquakes, and waves. This research provides an important reference for engineering construction.

2. Soil-fluid interaction

Based on Biot's consolidation theory [8], we can consider the soil-fluid interaction using Darcy's law. The response equation for the pore fluid can be formulated as

2.1. Seepage equation [9]

$$-\frac{\partial q_i}{\partial x_i}+q_v=\frac{1}{M}\frac{\partial P}{\partial t}+a\frac{\partial \varepsilon}{\partial t}-\beta\frac{\partial T}{\partial t} \tag{1}$$

Here, q_i is the seepage vector; q_v is the volumetric fluid source intensity; M is the Biot modulus; p is the pore water pressure; a is the Biot ratio; ε is the volumetric strain; T is the temperature; t is time and β is the coefficient of thermal expansion for the solid-fluid interaction. As the artificial island is at sea, its temperature change is relatively small, and has little effect on the stability, deformation, and structural forces. This article considers only the coupled actions of seepage, waves, and earthquakes, without considering the influence of the temperature; hence, $\partial T/\partial t=0$

2.2. Fluid-solid coupling equation [9]

$$\delta\sigma_{ij}+a\frac{\partial P}{\partial t}\delta_{ij}=H(\sigma_{ij},\varepsilon_{ij}-\varepsilon_{ij}^{T},\kappa) \tag{2}$$

Here，δ_{ij} is the Kronecker delta factor；σ_{ij} is the stress；$\delta\sigma_{ij}$ is the stress increment；ε_{ij} is the total strain； H_{ij} is from the given constitutive model； κ is a history parameter and ε_{ij}^{T} is the strain rate determined by temperature variation, for this scenario $\varepsilon_{ij}^{T}=0$.

3. Strength Reduction Method

Zheng [10, 11] used a new method, referred to as the strength reduction method, to calculate the slope's dynamic stability and consider the slope's dynamic characteristics under earthquake conditions. This method can fully describe soil tensile-shear failure during earthquakes. Traditional static slope stability analysis is based on the limit equilibrium method, and the safety coefficient w relating the anti-sliding force s and sliding force t is expressed as follows:

$$w = \frac{s}{t} = \frac{\int_0^l (c + \tan\varphi) dl}{\int_0^l \tau dl} \tag{3}$$

Here, c is the cohesion, φ is the angle of internal friction and τ is the dynamic shear stress. In the strength reduction method, the slope is made to approach the limit equilibrium state by reducing the shear strength of the soil as

$$c' = c / \omega, \quad \varphi' = \arctan(\tan\varphi / \omega) \tag{4}$$

where ω is the reduction parameter, which is the safety factor. c' and φ' are the values of c and φ after reduction, respectively.

However, slope failures under earthquake excitations are the result of both tensile and shear damage; hence, the tensile strength of the rock and soil mass should be considered. When using the strength reduction method, the tensile strength should also be reduced:

$$\sigma^{t'} = \sigma^t / w \tag{5}$$

Here, σ^t is the tensile strength and $\sigma^{t'}$ is the numerical value of σ^t after reduction.

4. **Test case**

4.1. Basic breakwater set-up

The environment of this breakwater features smooth ocean floors and a simple underwater landscape, which is composed of clay soil, backfill sand, and compaction sand, proportionately. The breakwater structure is composed of a plug-in steel cylinder structure. The steel cylinder is 40 m long, its thickness is 16 mm and its diameter is 22 m. The elevation of the cylinder head is 3.5 m, and the elevation of the cylinder base is -36.5 m. The top level of the soil layer is -8.5 m, and the water level is 2.57 m, as shown in Figure 1.

The numerical model is 190 m long, with a height of 80.5 m. The water level for the breakwater is 2.57 m, and the artificial pumping water level is -12.5 m on the inland side. To improve the calculation efficiency and reduce the grid size, a typical cross section was selected in calculation. The cross-sectional element was chosen to simulate the interactions between the cylinder and the surrounding soils. The backfill sand as well as compaction sand are considered as liquefiable soils, and the parameters are shown in Table 1.

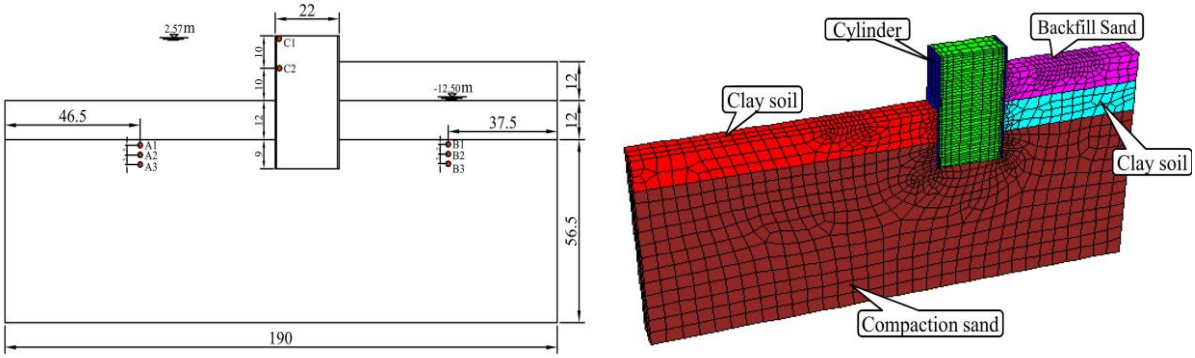

(a)Model dimensions (b) Calculation model

Figure 1. calculation model for the breakwater

Table 1. Geotechnical material parameters

Materials	Dry density kg/m^3	Elastic modulus /Mpa	Poisson's ratio	Angle of internal friction	Cohesivity /kPa
Backfill Sand	1380	40	0.35	30	4
Clay soil	1350	30	0.38	13	22
Compaction sand	1380	45	0.35	32	2
Cylinder	3500	2000	0.17	--	--

4.2. Input earthquake wave

The typical earthquake intensity is category VII in the project area, but considering the importance of its strategic location and economic status, category VIII is decided upon for the anti-seismic design. The peak amplitudes of the Kobe earthquake (Japan, 1995) were between 0.2 g and 0.3 g in numerical calculations. The input acceleration amplitude of 0.2 g was used to calculate the stress, acceleration response and stability of the breakwater. The input amplitudes from 0.2 g to 0.3 g were applied to analyze the liquefaction of the artificial island. The input acceleration waveform is shown in Figure 2.

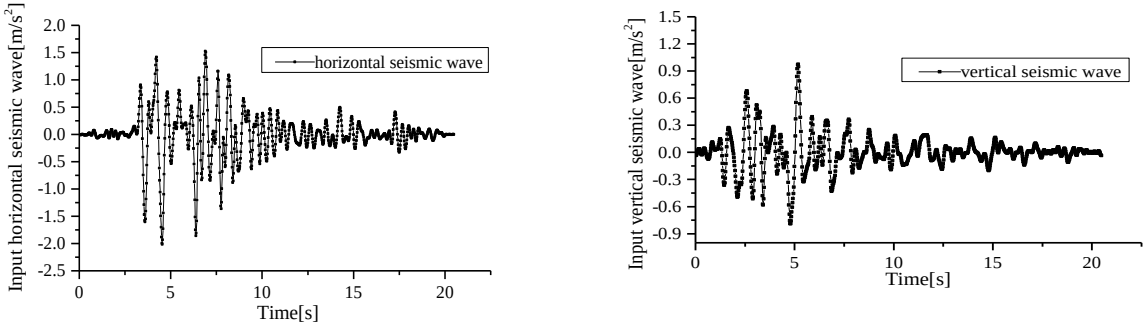

(a) Horizontal direction (b) Vertical direction

Figure 2. Put earthquake waves (Kobe wave)

4.3. Dynamic earth pressure

Monitoring points were set up at 3 m intervals on both sides of the steel cylinder to record the time-history curve of the dynamic earth pressure. The distribution of the dynamic earth pressure is shown in Figure 3.

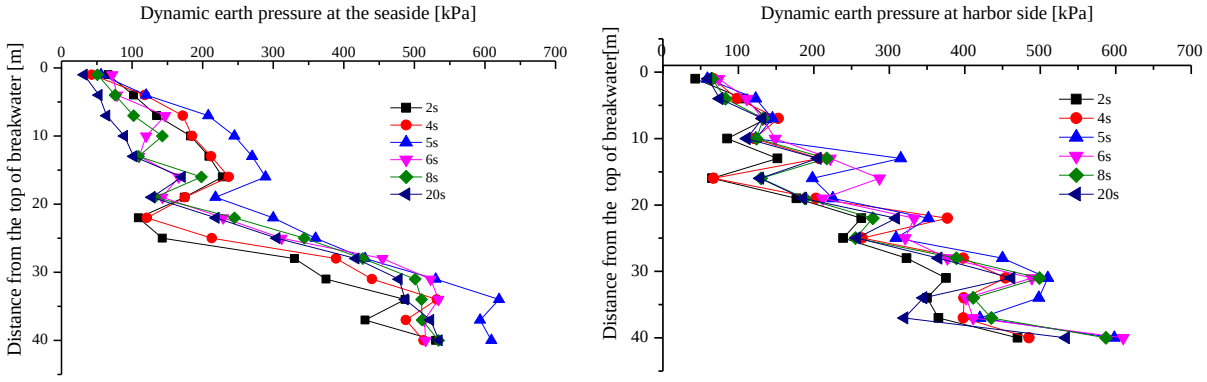

(a)Left-hand side of the breakwater (b) Right-hand side of the breakwater

Figure 3. Dynamic earth pressure distribution on both sides of the breakwater when triggered by an earthquake

Based on the dynamic earth pressure distribution on both sides of the breakwater under earthquake excitations (see Figure 3), it can be concluded that the deeper the buried depth of the breakwater, the greater the dynamic earth pressure. The pressure response on both sides of the breakwater is more notable between 4s and 6s under earthquake conditions.

4.4. Stability of the breakwater

The strength reduction method was used to find the dynamic stability of the artificial island. In this method, the artificial island was made to approach the limit equilibrium state by reducing the shear strength of the soil. When the reduction factor $\omega = 1.39$, the displacements of monitoring points C1 and C2 converged after the earthquake, so the breakwater was stable. When the reduction factor $\omega = 1.40$, the displacements of monitoring points C1 and C2 did not converge and would continue to increase after the earthquake, so the breakwater was not stable and entered the limit equilibrium state (as shown in Figure 4).

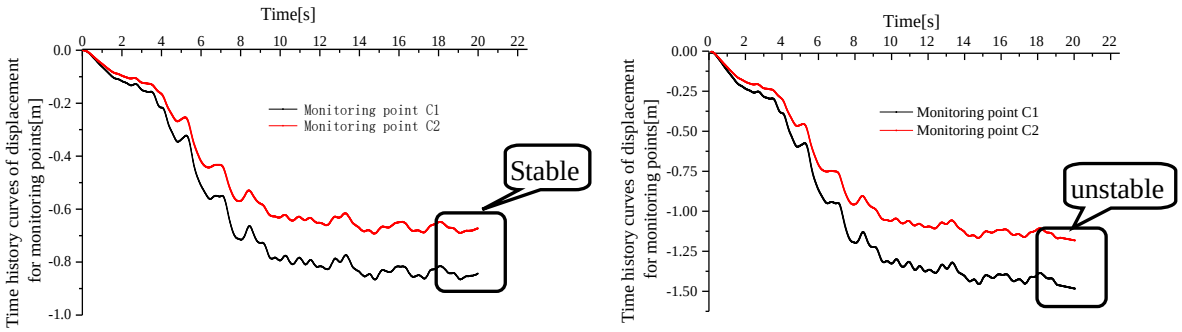

(a) Reduction factor of 1.39 (b) Reduction factor of 1.40

Figure 4. Horizontal displacement time-history curves of monitoring points under different reduction factors

From Figure 5, it can be seen that a displacement mutation occurs when the reduction factor $\omega = 1.40$, which shows the difference in stability occurring with a small change in reduction factor.

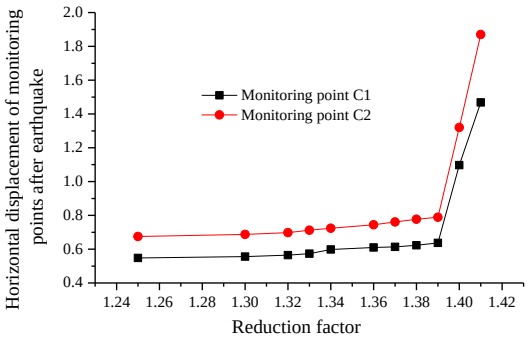

Figure 5. Reduction factor - Horizontal displacement curve

When the reduction factor $\omega = 1.40$, the plastic shear zones of the artificial island become connected, and the final failure surface of the artificial island can be seen as the red line shown in Figure 6. Based on the above analysis, the dynamic safety factor of the breakwater is found to 1.39.

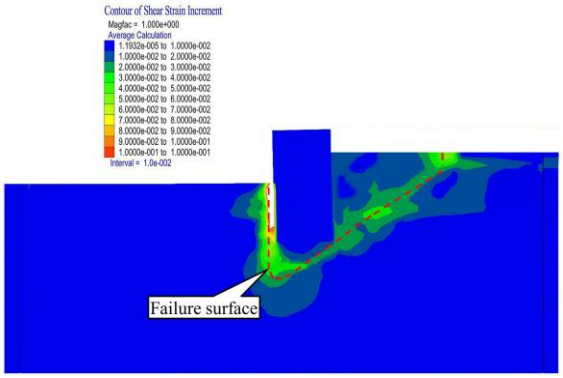

Figure 6. Plastic shear zone

5. Conclusions

(1) When the water level was increased to the design height, the dynamic safety factor of the breakwater calculated with the strength reduction method was 1.39, which meets the safety requirements. The final failure surface appeared at the breakwater-soil interface.

(2) The deeper the buried depth of the breakwater, the greater the dynamic earth pressure will be. The dynamic earth pressure response is more notable on both sides of the breakwater from 4 to 6 s under earthquake conditions.

(3) The dynamic safety factor of the breakwater, calculated using the strength reduction method, concerns the water levels. When the water level is pumped to the design height, it can meet the safety requirements. The ultimate failure surface appeared at the breakwater-soil interface.

Acknowledgements

This research was supported by the National Natural Science Foundation of China (51178457), National Natural Science Foundation of China (51378496), Natural Science Foundation of Chongqing City of China(CSTC2013jcyjys0002), Graduate Student Scientific Research Project of Chongqing City of China(CYB15108), and the Youth Foundation of Force Engineering University (2018QNJJ003).

References

[1] Wang Y L and Wu Z S 2013 *Risk Assessment for the Construction Drawing Design of the East and West Artificial Islands of Hong Kong-Zhuhai-Macao Bridge* CONSTRUCTION TECHNOLOGY 42 pp 64-68.

[2] Mnasri C, Hafsia Z, Omri M and Maalel K 2010 *A moving grid model for simulation of free surface behavior induced by horizontal cylinders exit and entry* Engineering Applications of Computational Fluid Mechanics 4 pp 260–275.

[3] Williams A N and Li W 2000 *Water wave interaction with an array of bottom-mounted surface-piercing porous cylinder* Ocean Eng. 27 pp 841-866.

[4] Bricker J D 2013 *Turbulence Model Effects on VOF Analysis of Breakwater Overtopping during the 2011 Great East Japan Tsunami* In Proceedings of the 35th IAHR World Congress, Chengdu, China.

[5] Mnasri C, Hafsia Z, Omri M and Maalel K 2010 *A moving grid model for simulation of free surface behavior induced by horizontal cylinders exit and entry* Engineering Applications of Computational Fluid Mechanics 4 pp 260–275.

[6] WANG L Y, JIANG P M and LIU H L 2011 *Mechanism analysis of residual liquefied deformation of breakwater during earthquake*, Rock and Soil Mechanics 31 pp 3556-2562.

[7] Matsuda T, Maeda K, Miyake M, Miyamoto J, Sumida H & Tsurugasaki K 2016 *Instability of a Caisson-Type Breakwater Induced by an Earthquake–Tsunami Event* International Journal of Geomechanics 16 pp C4016003.

[8] BIOT M A 1956 *General Solution of the Equation of Elasticity and Consolidation for a Porous Material* Journal of Applied Mechanics 23 pp 91-96.

[9] FLAC3D Fast Lagrangian Analysis in Three Dimensions User's Guide. Itasca Consulting Group, Minneapolis 2013.

[10] Lai J, Zheng Y R, Liu Y, Li X D and Liu H W 2016 *Seismic design of multiple anti-slide piles by strength reduction dynamics analysis method* Electronic Journal of Geotechnical Engineering 181 pp 1-10.

[11] ZHENG Y R, ZHAO S Y and ZHANG L Y 2002 *Slope stability analysis by strength reduction FEM* Engineering Science 4 pp 57-61.